

Wi-Fi HaLow Wildfire Sound Detector

Stefan Rizanov, Peter Yakimov

Faculty of Electronic Engineering and Technologies
Technical University of Sofia
8 Kliment Ohridski blvd., 1000 Sofia, Bulgaria
srizanov@tu-sofia.bg, pij@tu-sofia.bg

Abstract –The expanding severity and occurrences of wildfires has led researchers in search for new technologies and applying cutting-edge solutions for the early detection of such fire hazards. Within this work we propose a Wi-Fi HaLow wildfire sound detector. Described are the spectral specifics of forest fire noise, the Wi-Fi HaLow standard and its advantages. The prototyped system was subjected to tests - capturing real sound data from fire and non-fire events and distinguishing between them by means of sonogram analysis.

Keywords– audible noise, embedded system, forest fire noise, sound detection, wildfire, Wi-Fi HaLow

I. INTRODUCTION

Wildfire specifics, risk assessment and their detection have been at the focus of scientific and governmental research in recent times. Different technological solutions have been proposed over the years - from edge-computing sensory nodes which capture ambient environmental parameters, gas and emitted particulate concentrations; infrared and multi-spectral camera based solutions; satellite scanning systems; Unmanned Aerial Vehicle (UAV) and Unmanned Terrestrial Vehicle (UTV) sensory modules, controlled by qualified personnel or swarm-based self-organized systems. Wireless Sensor Nodes suffer from limited detection range capabilities. Infrared and multi-spectral cameras are difficult to automate, operate and generate large amounts of image data making wireless transfer more difficult. Satellite scanning systems have limited spatial and temporal resolutions and their deployment is extremely expensive. UAVs need operator oversight or complex self-organization algorithms, which necessitate the usage of hardware platforms with a higher computational capability and power-consumption, limiting the operational range of these systems. In the field of wireless sensory systems the main utilized standards are - GSM, Bluetooth, WiFiLoRa, ZigBee, NB-IoT, SigFox. For large amounts of data to be transferred - GSM and WiFi are typically used, with GSM modules having a large power consumption and requiring cellular coverage, whilst WiFi modules are limited in range up to 150m. All other communication standards are typically directed towards transferring smaller amounts of data, with Bluetooth being limited to roughly 150m connection distance, whilst LoRa, ZigBee, NB-IoT and SigFox allow for large communication ranges up to several kilometers between the end-devices. The goal of our work was to investigate and develop a novel technological sensory unit, based on sonogram extraction in order to overcome the disadvantages of the mentioned above methods. This approach will need transfer of large amounts of data and the general used standards will not be able to

ensure it. The proposed sensory node will capture environmental sounds in real time and transfers the data uplink over an established Wi-Fi HaLow wireless communication channel. Our preliminary scientific research showed that the Wi-Fi HaLow technology has not been utilized in past research works and its fusion with embedded audio sensing promises a novel IoT platform for wildfire early detection. Wi-Fi HaLow is a promising new technology which has the advantages of allowing larger amounts of data to be transferred over distances of several kilometers with a sufficiently lowered power consumption. The proposed research work is organized in the following manner: Chapter 2 presents an in-depth scientific review over the specifics of wildfire emitted sounds, their spectrum and the effects of flickering, crackling and fire size over the resultant audio profile (signature) of the forest fire event; Chapter 3 describes the Wi-Fi HaLow standard and its advantages over existing wireless communication technologies; Chapter 4 showcases the developed and prototyped embedded HaLow sound detector system, discussing some hardware and software design aspects of it; Chapter 5 presents a series of preliminary tests, which we performed as a proof-of-concept and in order to evaluate the developed system's capability to distinguish between fire and non-fire events, based on real measurement data, noise reduction and a subsequent transient data conversion into a linear and Mel spectrograms.

II. WILDFIRE-EMITTED SOUND

The resultant audio wave from a combustion process is an effect caused by the high temperature expansion of air in proximity to the fire source[1]. The spectrum of this acoustic wave is contained both within the infrasound and audible spectrums[1]. Wood combustion is a relatively slow process so its corresponding sound power is lower than other materials [1]. Sounds emitted by similar sources exhibit similar spectral characteristics[2]. The amount of available biomass fuel influences the sonogram of the emitted acoustic waves[3].

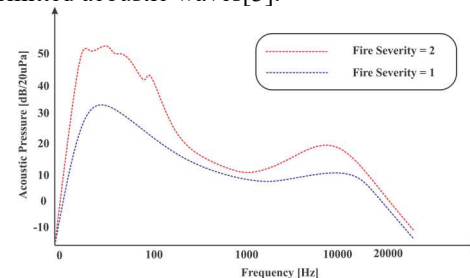


Fig. 1.Example audio sound spectrum for a wildfire

The noise spectra of different types of fires (surface and crown fires) vary - gradual increase of the trend line towards lower frequencies for surface wildfires and for crown wildfires a bell-shaped trend line can be observed[4]. Figure 1 shows an example audio spectrum for a wildfire with two severities.

When an increase in the severity of a wildfire is present the bell-shaped trend line is more clearly and distinctly observable[4]. From past combustion experiments, cited in literature, the emitted acoustic waves for paper and wood materials have a distinct spectrum with elevated spectral components within the frequency band of 20Hz-100Hz, peaks being observed at 20Hz, 50Hz and 100Hz[1]. The emission of acoustic waves equal in frequency to the flame flickering is due to the presence of rising flame rolls, which rise in a weakly explosive manner[3]. The flickering behavior of wildfires results in the emission of sound waves, whose frequency is related to the size of the burning surface[3]. An expansion of the size of the fire leads to a gradual decay in the flickering frequency[3]. In order for a flame to exhibit a flickering motion it has to expand in size beyond a certain threshold[3]. In past literature works it was defined that the flickering frequency is always less than 10Hz for all types of burning biomass or fuel materials[3]. In experiments aimed towards evaluating the sonogram of an ethanol fire, it was observed that maximum power was concentrated around the 2Hz frequency[3]. It was deduced that this corresponds to the fire flickering frequency[3]. In another research work it was stated that this flickering frequency is within the range 1Hz-100Hz and its value is inversely related to the square root of the circumference of the burning fuel surface[5]. Crackling audible pulse noises are generated within the high-frequency range due to microscopic changes in mechanical stress in materials, due to thermal gradients and amount of absorbed heat[5]. These crackling frequencies are within the range 3kHz-12kHz[5]. Every substance has a unique shadowed projective area and power of combustion[1]. Past research showed that for different kinds of burning biomass (straw, slash, shrubs, pinus needles) a large portion of the power of the emitted audio waves is located at the frequency range 0Hz-500Hz[5]. A characteristic spectral behavior for wildfire events is an elevated noise level at the low frequency band 0Hz-500Hz in respect to a non-fire baseline and an induced spike in the high-frequency 3kHz-12kHz audible band[5]. The peak of the audio wave power is centered around a low frequency, whose value is proportional to the severity of the wildfire event[6]. In addition the low-frequency bandwidth of the emitted sound is changed by the size of the wildfire - larger fires having a wider low-frequency emission band than smaller fires, which have a narrower band[6].

Some of the potential difficulties in performing audio spectrum analysis are that: 1) rain noise is a potential false positive error source, due to its similar spectrum to active wildfires; 2) infrasonic wave analysis is preferable due to the lack of audible background noise[1,4]. In addition pure flickering frequency analysis is prone to false positive detections [3].

The thermo-physical properties of the ambient environment also have to be taken under consideration

when performing spectrographic audio analysis of wildfire events. Thermal anomalies induce so-called atmospheric inhomogeneities[7]. The acoustic propagation velocity is influenced by the ambient conditions and can be calculated by the following formulas:

$$\overrightarrow{c_{eff}} = c\vec{n} + \vec{v} \quad (1)$$

$$c = 20.05\theta_v^{1/2} = 20.05\sqrt{\theta(1 + 0.61q)}, \quad (2)$$

where $\overrightarrow{c_{eff}}$ is the effective velocity of an acoustic ray, which propagates through the atmosphere; \vec{n} is the unit wave front normal; \vec{v} is the wind velocity; c is the sound speed; θ_v is the virtual temperature; θ is the potential temperature; q is the mixing ratio [7]. As it was described in the cited research - the propagation time is affected by the thermal pattern distribution and the fluidic motion in proximity to the acoustic wave's propagation path[7]. This effect can be modeled as a Doppler frequency shift as a function of temperature[7].

Wildfire audio sound analysis and classification through Machine Learning classical algorithms such as Support Vector Machines and Deep Neural Networks has shown a promising overall accuracy within the range 85%-93%[8]. In past scientific works, analysis and an evaluation of different Machine Learning algorithmic solution was based on using readily available audio tracks of wildfires. Available fire sounds can be found in the Forest Wild Fire Sound Dataset[2]. Pure sound waves are difficult to be integrated into automated recognition software, due to their complex nature, and this is the reason why converting the raw audio data into Mel spectrograms with inherently lower dimensionality and has been proposed in previous works [2]. Mel-scaled spectrograms are extracted spectrograms which pass through a set of Mel filter-banks (triangular filters), according to the Mel scale[8]. The Mel scale is related to subjective audible pitch perception, defining which audible tones are subjectively placed at equal distances from one another [8]. For any given frequency f the corresponding Mel_m value can be calculated by the formula:

$$m = 2595\log_{10}(1 + \frac{f}{700}) \quad (3)$$

III. THE WI-FI HALOW TECHNOLOGY

Wi-Fi HaLow is a new sub-gigahertz standard for wireless communication that incorporates the IEEE 802.11ah technology and it is certified by the Wi-Fi alliance and FCC (Federal Communications Commission). It operates in the unlicensed ISM band[9,10,11]. This technology utilizes narrow OFDM (Orthogonal Frequency Division Multiplexing) channels. The coding scheme utilizes BPSK, QPSK, 16-QAM and 64-QAM modulations, depending on the MCS index. The channel bandwidth is configurable to be: 1MHz; 2MHz; 4MHz; 8MHz; or 16MHz. The corresponding data rates for these channel configurations are: 333kbps-3.33Mbps; 722kbps-7.22Mbps; 1.5Mbps-15Mbps; 3.25Mbps-32.5Mbps; 8.67Mbps-86.7Mbps. It is aimed towards allowing long-distance data

changes at above 1km (up to 3km). This allows it to cover an area 100 times larger in size compared to 2.4GHz and 5GHz Wi-Fi networks. Its flexibility is in providing full native IP support and not necessitating the development of proprietary hubs and gateways. This allows for its eased integration into existing IP networks. The technology allows for up to 8191 devices to be supported by a single access point (AP). Wi-Fi HaLow utilizes also the Wi-Fi standard WPA3 security features. Additional emphasis is pointed towards the integration and availability of different data-transfer rates, as well as sleep and power management modes in order to optimize energy consumption and prolong the operational lifetime of battery-powered (energy limited) devices.

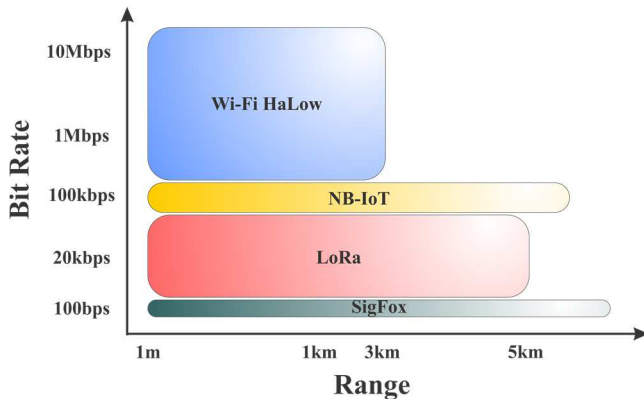


Fig. 2. Bit rates and data-exchange ranges for several long-range wireless standards

Figure 2 shows a diagram representation of the available bit rates and data-exchange ranges for several long-distance wireless standards.

Wi-Fi HaLow data rates are typically within the range of 150kbps - 15Mbps, which is roughly 600 times faster than LoRaWAN. HaLow supports bi-directional data exchange. In respect to power usage, when evaluating the bits per Joule, it is stated that Wi-Fi HaLow is 7 times more power efficient compared to LoRaWAN, due to the increased bit rates.

A successful video-call line-of sight connectivity test was performed by the company Morse Micro in San Francisco's Ocean Beach with a distance between the two end-devices of 3km. The available power on the receiving end can be calculated based on the Friis equation:

$$P_R = P_T \frac{G_T G_R \lambda^2}{(4\pi)^2 d^n}, \quad (4)$$

where P_R - power available from the receiving antenna; P_T - power supplied to the transmitting antenna; G_T - gain of the transmitting antenna; G_R - gain of the receiving antenna; λ - wavelength; d - distance; n - spatial coefficient.

IV. DEVELOPED HALOW WILDFIRE SOUND DETECTOR

The developed system is aimed towards providing an embedded IoT sensory unit, which would capture in real time the audible noise of its surrounding environment with several microphones and transferring the data upstream over an established Wi-Fi HaLow wireless communication

channel. The audio data then can be further stored and analyzed in real-time on the server's side by applying spectral identification methods, aimed towards distinguishing fire from non-fire events, based on their audio profile (signature). The goal of our work is to establish as a first step a sensory platform, which can be integrated in a broader and more complex network, whose operation and detection capability may be partially or fully automated, limiting or eliminating completely the necessity for operational observation oversight by qualified personnel. Figure 3 shows a rough representation for the application of the proposed system.



Fig. 3. Application of the proposed system

In order for us to develop such a system we started by selecting a proper wireless communication module, CPU and microphone sensor. Figure 4 shows a block diagram representation of the developed and prototyped system.

We integrated a computationally powerful ARM Cortex STM32F7xx CPU with DSP capabilities. For the Wi-Fi HaLow wireless module we implemented the currently first and only certified SoM (System-on-Module) SX-SDMAH by the Japanese company Silex Technology. The SX-SDMAH HaLow SoM integrates a MM6108 radio transceiver module by the company Morse Micro.

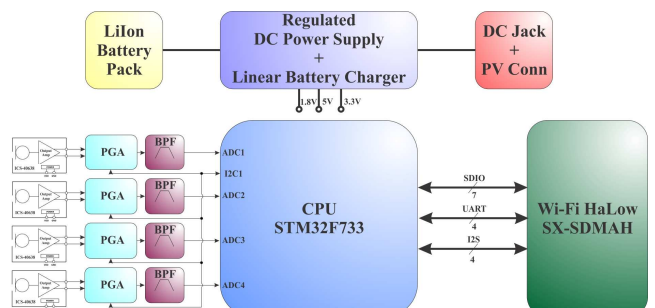


Fig. 4. Block diagram of the developed system

Silex Technology additionally offers the AP-100AH Wi-Fi HaLow Access Point, which can be used for the full system's integration. A photograph of the SX-SDMAH SoM and AP-100AH modules is shown in Figure 5.



Fig. 5. Photographs of the SX-SDMAH SoM and AP-100AH modules [10]

In order for us to be able to capture the audible sounds emitted by wildfires, we integrated 4x ICS-40638 microphones, which have a differential analog voltage output. Table 1 shows the typical values for the AOP (Acoustic Overload Point) and some other important parameters of the chosen microphones.

TABLE. 1. Parameters of the ICS-40638 microphone

Sensitivity	-44dBV \pm -42dBV
AOP	138dB
Bandwidth	35Hz \pm 20kHz
Dynamic Range	107dB
SNR	63dBA
THD	0.2%
PSRR	-111dBV

To expand the range, we added a I2C-configurable PGA (Programmable Gain Amplifier) and an active band-pass filter for the 4 microphone channels. The resultant analog voltages are fed to the CPU's ADC channels, configured to work in DMA mode. For the power supply portion of our design we integrated a Li-Ion battery pack, containing 3x18650 2.2Ah rechargeable battery cells from the company LG as well as a regulated DC/DC converter and linear battery charger IC. For the power charging input of the system we placed a DC power jack and a photovoltaic panel connector for future energy harvesting capability integration. In order to compress the captured audio sensory data, we decided on using the open-source Opus Audio Encoder, which is used in online platforms such as Skype[12].The Opus Encoder API is made publically available online. For our current state of system testing we configured the encoder with the following parameters: Bandwidth ->Fullband (up to 20kHz); Sample Rate -> 48kHz; Payload ->Frame_Size/4; Complexity ->8/10 (defines how complex the compressing encoding scheme is).

V. PRELIMINARY SPECTRAL TESTS

In order for us to test, evaluate and validate the functionality of our developed system we performed several preliminary on-site tests. The tests were aimed towards capturing audio sounds of different environmental surroundings, performed in a controlled manner. Of interest were a daytime campfire, nighttime campfire, forest environment with wind presence, rain and two larger controlled fires. The developed system was placed in a relatively close proximity of 5m to the built campfires and at a distance of 10m to the larger controlled fires. We captured the resultant audio noises as well as an additional reference noise track, which we used to evaluate in a quiet room the self-emitted audible noise from the prototyped system.

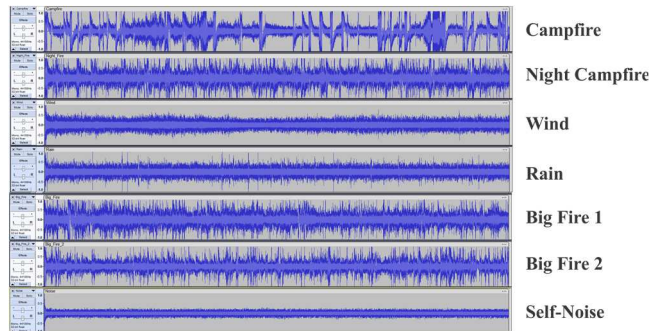


Fig. 6.Captured raw sound data

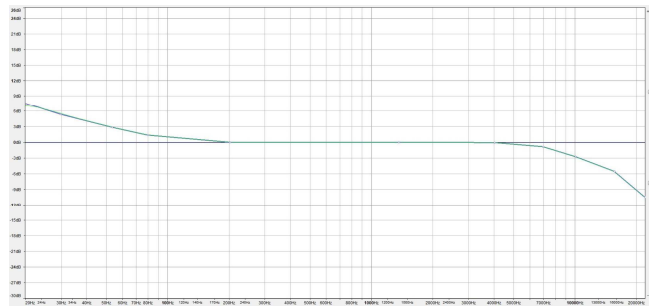


Fig. 7.Applied microphone non-linearity correction filter

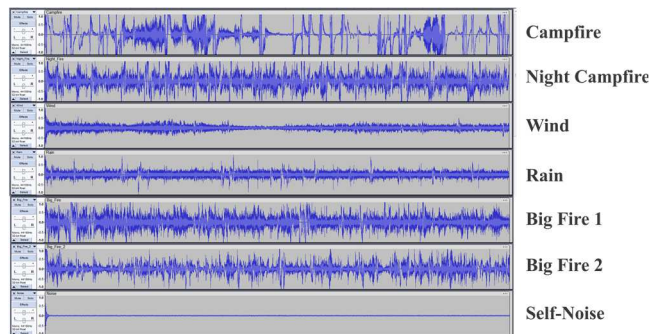


Fig. 8.Filtered sound data

We used this reference so called "self-noise" track for establishing the filter profile for the other captured audio tracks. Figure 6 shows the captured raw audio tracks from the carried out tests. Due to the fact that the used MEMS microphone is non-linear in the audible spectral band - we constructed and applied a correction filter, tailored to the parameters, listed in the microphone's documentation. The constructed non-linearity correction filter is shown in Figure 7. Using the Audacity software we performed a 20dB noise reduction with a sensitivity factor of 6 and 6 frequency smoothing bands, based on a snippet of the captured Self-Noise audio track. The resultant filtered audio tracks are shown in Figure 8.

In order for us to additionally evaluate the spectral characteristics of the captured audio tracks for the different events we visualized the data in a logarithmic and Mel spectrogram formats. Figure 9, Figure 10 and Figure 11 show respectively the linear, Mel and logarithmic spectrograms for the 6 performed tests.

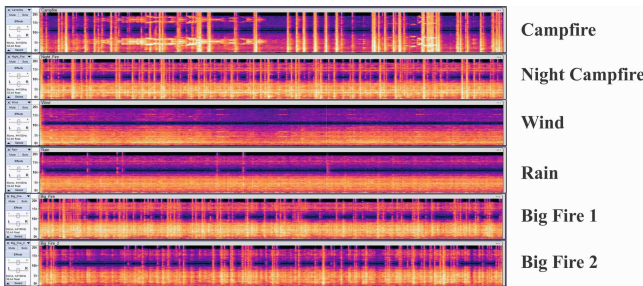


Fig. 9. Linear spectrograms of the captured sensory data

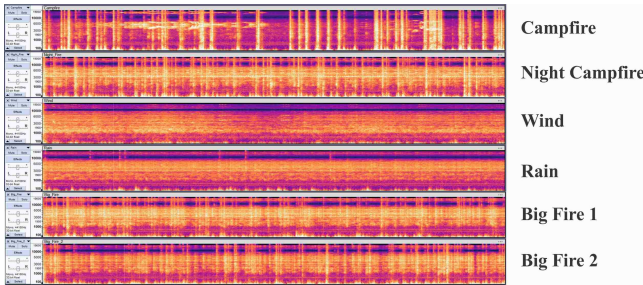


Fig. 10. Mel spectrograms of the captured sensory data

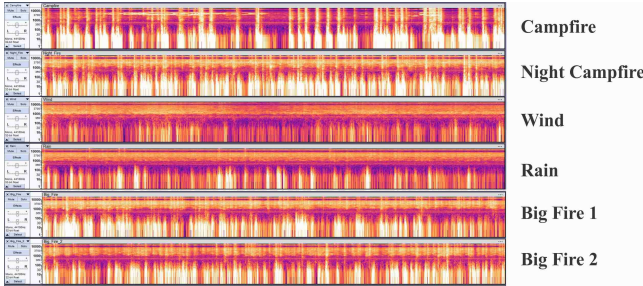


Fig. 11. Logarithmic spectrograms of the captured sensory data

As can be seen from the resultant spectrograms, there are distinct patterns and observable differences between the different captured audio tracks. The wind spectrograms have a characteristic monotonic spectrogram, without the presence of visible spectral lines. The rain spectrograms have small in number and narrow in width spectral lines. Campfire spectrograms have a visible presence of wider spectral lines but smaller in number than nighttime fires and big fires. Nighttime fires and big fires have a large number of spectral lines, which are narrow in width. The wind and rain tracks are easily distinguishable from the rest when using the Mel spectrograms, due to the fact that they are more fluent, with no visible spectral line patterns. A distinction between nighttime campfires and big fires is best performed by analyzing the logarithmic spectrograms, where larger differences can be observed. These resultant spectral images can potentially be used as data entries for the training and real-time automated distinction between fire and non-fire events by image classification and image recognition algorithms such as Convolutional Neural Networks (CNNs).

In order to evaluate whether the resultant spectrum of the captured fire and non-fire events is close to that of the data, reported in past scientific literature - we performed an FFT analysis over the captured acoustic sounds. The results for the logarithmic and linear FFT spectrum plot are shown respectively in Figure 12 and Figure 13.

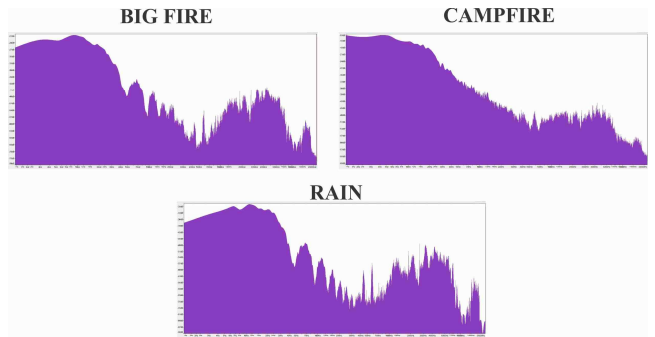


Fig. 12. Logarithmic FFT spectrum plot of the captured sounds

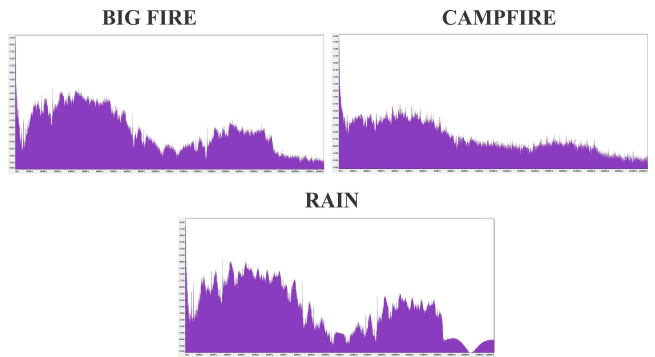


Fig. 13. Linear FFT spectrum plot of the captured sounds

Our findings showed that the FFT-derived spectrum data is in accordance with the results in past scientific works which discuss this topic. There is an observable double bell shaped curve form in the spectrum, with the bell peak difference being more distinguishable for larger fires compared to that of smaller fires. Additionally we confirmed that a non-fire event such as rain sounds have a similar in shape spectrum to that of large fires, making them more difficult to differentiate. Because of this reason we directed our interest towards numerically evaluating the resultant spectrums by calculating an average sound level for 3 spectral bands, which can be derived - 1Hz-1kHz; 1kHz-1.5kHz and 1.5kHz-20kHz, which we labeled respectively as BAND 1, BAND 2 and BAND 3. BAND 1 is representative of the low-frequency spectral bell, BAND 2 represents the plateau between the two bells, BAND 3 represents the high-frequency spectral bell.

TABLE. 2. Captured average sound levels for 3 spectral bands

	BAND 1 1Hz - 1kHz	BAND 2 1kHz - 1.5kHz	BAND 3 1.5kHz - 20kHz
Big Fire	-50dB	-70dB	-63dB
Campfire	-50dB	-62dB	-60dB
Rain	-60dB	-84dB	-72dB

TABLE. 3. Differences between spectral bound acoustic levels

	BAND 1 - BAND 2	BAND 1 - BAND 3	BAND 2 - BAND 3
Big Fire	20dB	13dB	7dB
Campfire	12dB	10dB	2dB
Rain	24dB	12dB	12dB

Table 2 and Table 3 present the resultant measurements. Our interest was whether the differences in sound levels in these 3 spectral bands can be used as a means to distinguish between these events and proposing a methodology through which this can be done in an automated manner. We will direct our analysis towards: 1) distinguishing between a small fire and a big fire; 2) small fire and rain; 3) big fire and rain. For the first presented task it can be seen that large fires have a comparatively larger $|BAND1 - BAND2|$ difference than campfires. Additionally campfires have noticeable small in value difference $|BAND2-BAND3|$. For the second task the $|BAND1 - BAND2|$ difference is best suited for distinguishing between a campfire and a rain event. For the third and most complicated task - our results showed that big fires have a gradual drop in difference values for the $|BAND1-BAND2|$, $|BAND1-BAND3|$ and $|BAND2 - BAND3|$ of roughly 6dB, whereas this gradual decay in acoustic level differences for the 3 evaluated parameters is not observed in rain events. In rain event it can be seen that there is a close to zero in value difference between the calculations for $|BAND1 - BAND3|$ and $|BAND2 - BAND3|$. This is why we propose that this decaying trend in the three parameter values is indicative of a big fire event, whilst additionally a very small difference between the $|BAND1 - BAND3|$ and $|BAND2 - BAND3|$ calculations and lack of gradual decay is indicative of a non-fire rain event. Our findings showed that just purely evaluating the difference between the captured sound levels for the peaks of the low-frequency and high-frequency bells is not sufficiently accurate for distinguishing between fire and non-fire events.

VIII. CONCLUSIONS

Within this work we have investigated and proposed the construction of a novel Wi-Fi HaLow wildfire sound detector embedded system. We performed an in-depth review over the topic of wildfire emitted sounds, their spectral specifics and effects such as flickering and cracking over them. We investigated the Wi-Fi HaLow technology and outlined its advantages over existing wireless communication standards. We performed preliminary evaluation tests of our system in order to determine whether it can distinguish between fire and non-fire events, based on captured audible transient data and a subsequent spectrogram conversion. The performed tests showed promising results and the authors' team efforts will be further directed towards expanding the system's detection capabilities and submitting it to more comprehensive and varied testing procedures and operational environments .

ACKNOWLEDGEMENT

The presented results within the current scientific publication are financed by the internal PhD-student aiding projects of the Technical University of Sofia for 2023. The project identifier is № 232ПД0005-03.

REFERENCES

- [1] Guan, H., Fang, S., & Jiang, J. X. (2013, July). The Detection and Analysis of the Combustion Audio. In 2nd International Conference on Science and Social Research (ICSSR 2013) (pp. 795-798). Atlantis Press.
- [2] Huang, H. T., Downey, A. R., & Bakos, J. D. (2022). Audio-Based Wildfire Detection on Embedded Systems. *Electronics*, 11(9), 1417.
- [3] Schultze, T., Kempka, T., & Willms, I. (2006). Audio-video fire-detection of open fires. *Fire safety journal*, 41(4), 311-314.
- [4] Khamukhin, A. A., Demin, A. Y., Sonkin, D. M., Bertoldo, S., Perona, G., & Kretova, V. (2017). An algorithm of the wildfire classification by its acoustic emission spectrum using Wireless Sensor Networks. In *Journal of Physics: Conference Series* (Vol. 803, No. 1, p. 012067). IOP Publishing.
- [5] Viegas, D. X., Pita, L. P., Nielsen, F., Haddad, K., Tassini, C. C., D'Altrui, G., ... & Tsangaris, H. (2008). Acoustic characterization of a forest fire event. *WIT Transactions on Ecology and the Environment*, 119, 171-179.
- [6] Zhang, S., Gao, D., Lin, H., & Sun, Q. (2019). Wildfire detection using sound spectrum analysis based on the internet of things. *Sensors*, 19(23), 5093.
- [7] Sahin, Y. G., & Ince, T. (2009). Early forest fire detection using radio-acoustic sounding system. *Sensors*, 9(3), 1485-1498.
- [8] Peruzzi, G., Pozzebon, A., & Van Der Meer, M. (2023). Fight fire with fire: Detecting forest fires with embedded machine learning models dealing with audio and images on low power iot devices. *Sensors*, 23(2), 783.
- [9] <https://www.wi-fi.org/discover-wi-fi/wi-fi-certified-halow>
- [10] <https://www.silextechnology.com/wi-fi-halow-pillar>
- [11] <https://www.morsemicro.com/>
- [12] <https://opus-codec.org/>